

# UNIVERSITÀ DEGLI STUDI DI PADOVA

**Dipartimento di Fisica e Astronomia "Galileo Galilei"**

**Corso di Laurea in Fisica**


**Tesi di Laurea**

## Superfluorescence Dynamics in Er:YLF


**Relatore**

**Dr. C. Braggio**

**Laureando**

**Alexey Vladimirovic Bortoli Saygashev**


**Anno Accademico 2018/2019**

# Contents

**1 Introduction** **1**

**2 An elementary theory of superradiance** **3**
2.1 Spontaneous emission in a two atoms system for $d \ll \lambda$ . . . . . 3
2.2 Extension to $N$ atoms . . . . . 5
2.2.1 Time profile of emitted intensity in superradiance . . . . . 6
2.2.2 Interatomic correlation . . . . . 7
2.3 The spacial extension of superradiance: the superfluorescence. The pencil-shaped sample 8
2.4 The influence of dephasing on superfluorescence . . . . . 9
2.5 Rare-earth elements . . . . . 9
2.5.1 $Er^{3+}$:YLF crystal . . . . . 10

**3 Experimental** **11**
3.1 Description of experimental setup . . . . . 11
3.2 Data analysis . . . . . 13
3.2.1 Peak detection and cutting . . . . . 13
3.2.2 Ringing elimination . . . . . 13
3.2.3 $\mu, \Gamma$ parameters estimation . . . . . 14
3.2.4 Peak interpolation . . . . . 14
3.2.5 Estimation of emitted photon number . . . . . 15
3.2.6 Square dependence . . . . . 15
3.2.7 $\tau_R$ dependence . . . . . 15

**4 Conclusions** **19**

# Chapter 1

# Introduction

Spontaneous decay is a phenomenon that has been described for the first time by Dirac, Wigner and Weisskopf, at the early ages of the development of quantum electrodynamics [5,6]. The theory is applicable to a multi-body system only when atoms don't interact during their decay. Dicke introduces in his seminal paper the case where this assumption doesn't hold [1].

The results he obtains not only tell that the system emits pulses, but the pulse duration now depends on $1/N$, where $N$ is the number of participating atoms to the process. The pulses temporal profile is described by a squared hyperbolic secant function. The resulting emission intensity scales as $N^2$. The atomic system radiates more intensively than the ordinary fluorescent emission, this is the reason why the process is called superradiance, or by a generalization to extended systems, superfluorescence. The superradiant emission has preferential escape directions, depending on the atomic sample shape (Figure 1.1).

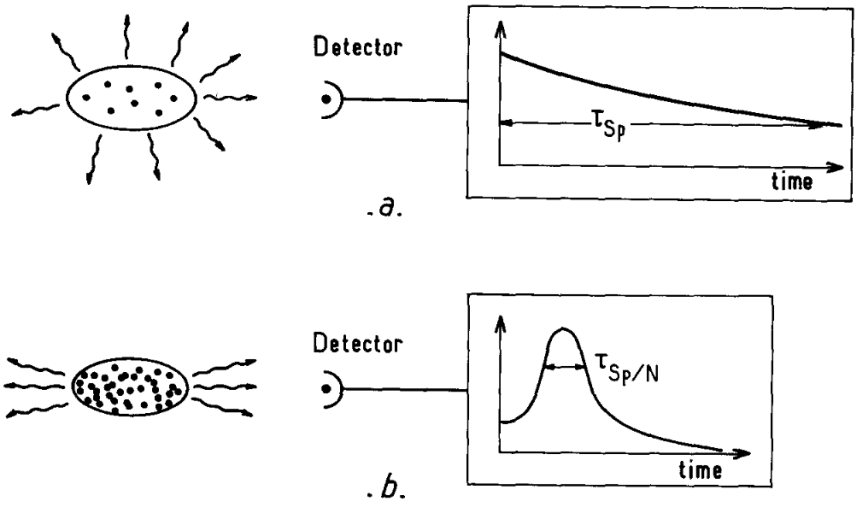


Figure 1.1: Comparison between standard fluorescence and superradiance. The main difference between two emission types are the directionality and intensity time evolution of the pulse. The ordinary fluorescence is isotropic while the superfluorescent emission shows radiation lobes. Moreover, the ordinary spontaneous emission follows the exponential decay with a constant $\tau_{sp}$ time while the superfluorescent pulse has a squared hyperbolic secant pattern and a $1/N$ time width, with $N$ the number of atoms. [3]

Superradiance is a collective process and it takes place when the group of excited atoms is left unperturbed during the formation of of the macroscopic dipole. A fundamental difference compared to the spontaneous and stimulated emission processes is that all atoms act together as a single entity and it isn't possible to identify single atoms.

This remarkable behaviour is manifest when the atomic coherence of the system, while influenced by environmental interactions that cause dephasing in atoms, persists for a sufficient interval of time.

Typical dephasing mechanisms, such as collisions in gases or lattice phonon interactions in crystals, make its experimental observation difficult. A possible solution to this problem is the use of optical crystals doped with rare-earths that are characterized by long and narrow levels lifetimes.

—

The superfluorescent bursts are the starting point of my work; data are taken from a quantum optics experiment in the INFN Legnaro National Laboratory (Padova).

I have fitted the electric signals recorded at a photodiode of superfluorescent pulses and have verified the typical squadred hyperbolic secant form expected from superfluorescence. With the fitted data I have shown the $N$-squared dependence of the photon burst intensity and the dependence of the pulse width following $1/N$. I have shown that these results are almost independent on the input laser pump power and have made an estimate of participating atoms contributing to the superfluorescent emission with the result of order of $10^{11}$ units.

# Chapter 2

# An elementary theory of superradiance

In this part I will describe superfluorescence from a theoretical point of view using the semiclassical formalism [1–3], namely using a quantum description of the atomic system and treating classically the radiation.

I start by considering the decaying rate of a two-level, two isolated atoms system at a distance less than the radiation emission wavelength ($d \ll \lambda$) and compare it with a system of two uncorrelated spontaneously emitting atoms (section 2.1).

I then extend the results obtained in the previous section by considering a system of $N$ coherently emitting atoms (section 2.2). By focusing on the dynamics of the radiation emission in subsection 2.2.1, I show the main characteristics of a superradiant emission: (i) $N^2$ dependence of the coherent pulses intensity on the number of participating atoms $N$, (ii) the temporal profile of the output pulses, (iii) and $1/\sqrt{N}$ dependence of the pulses duration $\tau_R$; in subsection 2.2.2 I consider interatomic correlations of the system.

I consider the pencil-shaped case in section 2.3 and explain how the geometry affects the superfluorescence emission dynamics.

In section 2.4 I briefly talk about the role of dephasing on the system and show the necessary conditions to observe superfluorescent emission. Such conditions can be satisfied in rare-earth doped materials and spectroscopic properties that are crucial in dephasing are detailed [4]; I briefly conclude focusing on $Er^{3+}$:YLF crystal, which has been used in the experimental part of this work.

## 2.1 Spontaneous emission in a two atoms system for $d \ll \lambda$

Let us consider a system of identical two atoms with two levels; their distance is far less than the radiation emission wavelength, $d \ll \lambda$, and this condition translates to coherent interaction via electromagnetic dipolar emission. We suppose at this level that atoms do not de-excite via other channels. We are going to see the temporal intensity profile $I(t)$ of the emission differs substantially from the case of two non correlated atoms.

The system has three energy eigenstates: $|ee\rangle, |m\rangle, |gg\rangle$, with $|m\rangle$ being a superposition of symmetrical ($|s\rangle = |ge\rangle + |eg\rangle)/\sqrt{2}$ and antisymmetrical $|a\rangle = (|ge\rangle - |eg\rangle)/\sqrt{2}$ states; by applying the spontaneous emission rate formula [5, 6]

$$\Gamma_{sp} = \frac{4}{3\epsilon_0 \hbar} \left(\frac{\omega_0}{c}\right)^3 \mathcal{D}^2 \tag{2.1}$$

it is possible to calculate the decay rate of the system. By calculating matrix elements of dipole interaction operators on atoms 1 and 2, $\mathcal{D}_1$ and $\mathcal{D}_2$ [2]:

$$\langle ee|\mathcal{D}_1+\mathcal{D}_2|s\rangle = \langle s|\mathcal{D}_1+\mathcal{D}_2|gg\rangle = \mathcal{D}\sqrt{2}$$
$$\langle ee|\mathcal{D}_1+\mathcal{D}_2|a\rangle = \langle a|\mathcal{D}_1+\mathcal{D}_2|gg\rangle = 0$$

or, by using spontaneous emission formula (Equation 2.1):

$$\Gamma_{ee,s} = \Gamma_{s,gg} = 2\Gamma$$
$$\Gamma_{ee,a} = \Gamma_{a,gg} = \Gamma_{ee,gg} = 0$$

The probability $P(t)$ of a transition in a spontaneous decay is found by solving:

$$\frac{\mathrm{d}P(t)}{\mathrm{d}t} = -\Gamma P(t)$$

which follows to an exponential law

$$P(t) = e^{-\Gamma t}$$

In case of two atoms system, by using the found rates, following equations for probability of each state can be written

$$\frac{\mathrm{d}P_{ee}(t)}{\mathrm{d}t} = -2\Gamma P_{ee}(t)$$
$$\frac{\mathrm{d}P_{s}(t)}{\mathrm{d}t} = -2\Gamma P_{ee}(t) - 2\Gamma P_{s}(t)$$
$$\frac{\mathrm{d}P_{a}(t)}{\mathrm{d}t} = 0$$
$$\frac{\mathrm{d}P_{gg}(t)}{\mathrm{d}t} = -2\Gamma P_{s}(t)$$

The resulting probability is therefore:

$$P_{ee}(t) = e^{-2\Gamma t}$$
$$P_{s}(t) = 2\Gamma t e^{-2\Gamma t}$$
$$P_{a}(t) = 0$$
$$P_{ee}(t) = 1-(1+2\Gamma t)e^{-2\Gamma t}$$

And the average photon emission intensity $I(t)$:

$$\begin{aligned} I(t) &= \Gamma_{ee,s}P_{ee}(t) + \Gamma_{s,gg}P_s(t) \\ &= 2\Gamma(1+2\Gamma t)e^{-2\Gamma t} \end{aligned}$$

This result says that the coherent spontaneous emission of two atoms has a fundamentally different time profile when compared with the spontaneous emission of two isolated atoms, which is:

$$I(t) = 2\Gamma e^{-\Gamma t}$$

In case of $N$ atoms the difference in this behaviour becomes even more relevant, as described in the section 2.2.

## 2.2 Extension to $N$ atoms

By modelling the free Hamiltonian $H_{f,i}$ of each atom of the system, labelled by $i = 1, 2, \ldots, N$, as a two-level system

$$H_{f,i} = \begin{bmatrix} \frac{1}{2}\hbar\omega_0 & 0 \\ 0 & -\frac{1}{2}\hbar\omega_0 \end{bmatrix} \tag{2.2}$$

it is possible to define $|e\rangle, |g\rangle$ as excited and ground states of each atom, with $\hbar\omega_0$ the difference of energy between $|e\rangle$ and $|g\rangle$ states.

Raising and lowering operators are introduced as follows

$$D_i^+ = |e\rangle\langle g| \qquad D_i^- = |g\rangle\langle e| \tag{2.3}$$

as well as diagonal operator

$$D_{3i} = \frac{1}{2}(|e\rangle\langle e| - |g\rangle\langle g|) \tag{2.4}$$

that satisfy the following commutation rules

$$[D_{3i}, D_j^\pm] = \pm\delta_{ij} D_i^\pm \qquad [D_i^+, D_j^-] = 2\delta_{ij} D_{3i} \tag{2.5}$$

In order to describe the system collectively we should make an important but quite restrictive assumption that holds in few cases but allows to understand the main properties of the superfluorescent system we are going to discuss.

The property is *the symmetry by particle exchange inside the system.*

In order to satisfy it, all atoms partecipating to the process should feel the same field the system is going to generate; thus, atoms should be confined in a little volume of space not be affected by time-delay effects of field propagation; in particular the region length $L$ should be far less than the generated radiation wavelength:

$$L \ll \lambda. \tag{2.6}$$

This is the so-called *Dicke superradiance model* [1]. Superfluorescence, on the other hand, is a process that acts on an extended body; however, most of the underlying physics doesn't change.

Now it is possible to describe the system of $N$ particles by introducing the system state vector

$$|e, e, \ldots e\rangle = \bigotimes_{i=1}^{N} |e\rangle \tag{2.7}$$

By comparing $D_i^+, D_i^-, D_{3i}$ with $\sigma^+, \sigma^-, \sigma_3$ Pauli matrices it can be shown the system behaves like a collection of $N$ spin-$\frac{1}{2}$ entities; this allows to describe the state of the system by using $|JM\rangle$ ket, where $J = \frac{N}{2}$ interpreted as total angular momentum.

The state $|JM\rangle$ is a fully symmetrical and is obtained by applying symmetrization operator on $J+M$ excited and $J-M$ ground-state particles:

$$|JM\rangle = S\,|\underbrace{e, e, \ldots, e}_{J+M}, \underbrace{d, d, \ldots, d}_{J-M}\rangle \tag{2.8}$$

that's possible because of assumptions on particle exchange symmetry.

By introducing collective operators

$$D^\pm = \sum_i D_i^\pm \tag{2.9}$$

$$D_3 = \sum_i D_{3i} \tag{2.10}$$

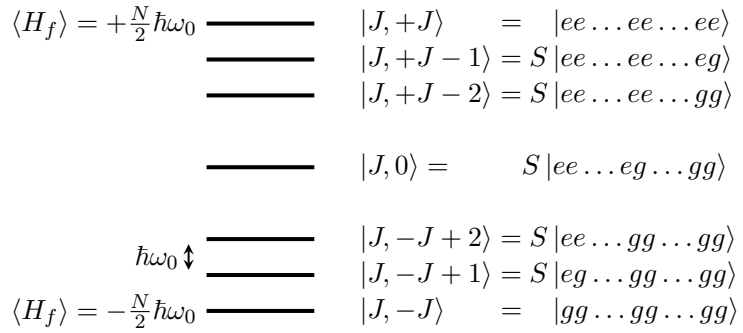


Figure 2.1: Superradiance model, described by ladder representation

$$D^2 = \frac{1}{2}(D^+D^- + D^-D^+) + D_3^2 \tag{2.11}$$

it is possible to define $|JM\rangle$ states by their eigenvector relationships

$$D_3\,|JM\rangle = M\,|JM\rangle \tag{2.12}$$
$$D^2\,|JM\rangle = J(J+1)\,|JM\rangle \tag{2.13}$$

and describe the action of ladder operators $D^+, D^-$ on them

$$D^+\,|J,M\rangle = \sqrt{(J-M)(J+M+1)}\,|J,M+1\rangle \tag{2.14}$$
$$D^-\,|J,M\rangle = \sqrt{(J-M+1)(J+M)}\,|J,M-1\rangle \tag{2.15}$$

The Hamiltonian of free atoms of the system now can be written as

$$H_f = \hbar\omega_0 \sum_{i=1}^{N} D_{3i} = \hbar\omega_0 D_3 \tag{2.16}$$

and the energy of state as $|JM\rangle$

$$\langle JM|H_f|JM\rangle = \hbar\omega_0 M \tag{2.17}$$

The description of the electromagnetic coupling among atoms is approximated to dipole interaction, so we define the interaction Hamiltonian as

$$H_{int} = -\mathcal{E}\mathcal{D} = -\mathcal{E}\sum_{i=1}^{N}\mathcal{D}_i = -\mathcal{E}d\sum_{i=1}^{N}(D_i^+ + D_i^-) = -\mathcal{E}d(D^+ + D^-) \tag{2.18}$$

The evolution of the system follows a ladder progression of $N+1$ levels, as shown in Figure 2.1 through the diseccitation of atoms; only dipolar interaction happens in the model, this way the only possible transitions are those that raise or lower one atom for each absorbed or emitted photon: $\Delta M = \pm 1$.

### 2.2.1 Time profile of emitted intensity in superradiance

To calculate transition rate $\Gamma_{M,M-1}$ between states $|J,M\rangle$ and $|J,M-1\rangle$ we consider dipole transition matrix $\mathcal{D}$ and spontaneous transition rate [5, 6]

$$\Gamma_{sp} = \frac{4}{3\epsilon_0\hbar}\left(\frac{\omega_0}{c}\right)^3 \mathcal{D}^2 \tag{2.19}$$

so we can write

$$\mathcal{D}_{M,M-1} = d\,\langle J,M-1|(D^+ + D^-)|J,M\rangle = \\ = d\sqrt{(J-M+1)(J+M)} \tag{2.20}$$

and calculate its matrix elements

$$\Gamma_{M,M-1} = \Gamma_{sp}(J - M + 1)(J + M) \tag{2.21}$$

We observe that for $M \approx 0$ the emission rate of the system is proportional to $N^2$.

At this point we can evaluate $I(t)$, the mean intensity of emitted photons when the system decays. Since the interaction is approximated as dipolar it is assumed that each transition takes place via emission of a single photon with a transition rate $\Gamma_{M,M-1}$. We can consider the mean total emission time of $n = J - M$ decayed photons as

$$\bar{t}(n) = \sum_{M=J-n+1}^{J} \Gamma_{M,M-1}^{-1} \tag{2.22}$$

by using Equation 2.21 and replacing the sum with the integral, while considering $J$ large enough we get

$$\bar{t}(n) = \Gamma^{-1} \int_{J-n}^{J} \frac{dM}{(J - M + 1)(J + M)} \tag{2.23}$$

Solving Equation 2.23 is possible to explicitly write the number of decayed atoms as $n(\bar{t})$

$$n(\bar{t}) = J + J \tanh[\Gamma J(\bar{t} - t_D)] \tag{2.24}$$

$$t_D = \frac{1}{\Gamma} \frac{\ln(2J)}{2J} \tag{2.25}$$

At this point we are able to describe the mean radiation intensity as function of time, where the mean time $\bar{t}$ is replaced by $t$ and $J = \frac{N}{2}$:

$$\frac{\bar{I}}{\hbar\omega_0} = \frac{\mathrm{d}n(t)}{\mathrm{d}t} = \Gamma \frac{1}{4} N^2 \operatorname{sech}^2 \left[ \Gamma \frac{1}{2} N (t - t_D) \right] \tag{2.26}$$

$$t_D = \frac{1}{\Gamma} \frac{\ln N}{N}. \tag{2.27}$$

This result shows strong differencies in a cooperative spontaneous emission, compared with ordinary fluorescence:

- The pulse form in time is a hyperbolic secant squared, compared to a decreasing exponential;
- The pulse duration now is proportional to $N^{-1}$, it results in a faster emission in case of more participating atoms; in the ordinary case the pulse time is independent of $N$;
- The pulse maximum intensity is proportional to the square of emitting units $N^2$, instead of just to their number $N$.
- Now there is a delay time ($t_D$) during which a macroscopic dipole build up.

### 2.2.2 Interatomic correlation

The correlation part plays an important role as the emission is coherent and most of atoms of the ensemble should participate to the superradiant process to obtain the square dependence as provided in Equation 2.21.

To evaluate the correlation between atoms we are going to estimate the value of $\langle JM|D_i^+ D_j^-|JM\rangle$. Let's start by considering

$$\langle JM|D^+ D^-|JM\rangle = \langle JM|\sum_{i\neq j} D_i^+ D_j^-|JM\rangle + \langle JM|\sum_i D_i^+ D_i^-|JM\rangle$$

from Equation 2.14, Equation 2.15 we get

$$\langle JM|D^+D^-|JM\rangle = (J-M+1)(J+M)$$

while

$$\langle JM|\sum_i D_i^+ D_i^-|JM\rangle = \langle JM|\sum_i D_i^2 - D_{3i}^2 + D_{3i}|JM\rangle = J+M$$

using the symmetry by exchange on particles it's possible to write

$$\langle JM|\sum_{i\neq j} D_i^+ D_j^-|JM\rangle = N(N-1)\langle JM|D_i^+ D_j^-|JM\rangle$$

finally obtaining, by rearrangement

$$\langle JM|D_i^+ D_j^-|JM\rangle = \frac{J^2-M^2}{N(N-1)} \tag{2.28}$$

We can observe that when $M \approx 0$ and the system irradiates with rate proportional to $N^2$ the correlation between pairs of atoms, in mean, is maximum with value $\langle JM|D_i^+ D_j^-|JM\rangle \approx \frac{1}{4}$.

## 2.3 The spacial extension of superradiance: the superfluorescence. The pencil-shaped sample

From this moment it is necessary to consider the atomic system under study as spacially extended; Equation 2.6 doesn't hold anymore and all assumptions based on this hypothesis are not valid. In order to describe the considered system, quantization of electromagnetic field is required, as well as considerations on atomic distribution and evolution of field variables in quantum domain (Maxwell-Bloch and master equations). This description is provided by a more extended bibliographic material [2], [3], [7].

A realistic and quite general approximation of a common case superfluorescent system is named *pencil shaped sample* case, in which longitudinal size of active part of the atomic ensemble ($L$) is far greater than the transversal one ($2w$).

$$L \gg w \gg \lambda \tag{2.29}$$

Moreover geometric conditions are modelled by assuming Fresnel numbers close to one

$$F = \frac{\pi w^2}{L\lambda} \approx 1 \tag{2.30}$$

which allows to have a balance between a single diffraction mode of emission and not having too much divergent transverse field; in this case it's possible to treat the problem approximately as one dimensional and ignore transversal effects [3, p. 335]

With all these assumptions it is possible to define a constant $\mu$ that takes in account the effects of the extended geometry:

$$\mu = \frac{3}{8\pi}\Omega_0 \tag{2.31}$$

with $\Omega_0 = \lambda^2/\pi w^2$, which is diffraction solid angle of emitted dipolar radiation, that influences the emission rate $\Gamma N$ by changing it to $\mu\Gamma N$.

By introducing

$$\tau_R = \frac{1}{\mu\Gamma N} \tag{2.32}$$

we get from Equation 2.26

$$\frac{I}{\hbar\omega_0} = \frac{N^2\mu\Gamma}{4}\operatorname{sech}^2\left[\frac{1}{2\tau_R}(t-t_D)\right] \tag{2.33}$$

## 2.4 The influence of dephasing on superfluorescence

The theory considered until now has assumed an interatomic distance far less than the radiation wavelength or a perfectly symmetric configuration among atoms, which are ideal conditions for the generation of a superfluorescent beam; in practical cases the symmetry requirements are never perfectly satisfied. The consequence is the dephasing of atomic Bloch vectors of the system; this takes place because dipole-dipole interactions between atoms causes shifts of atomic energy levels. In addition possible local asymmetries of the field affect the coherence of atoms and consequently the construction of a macro-dipole that pre-exists superfluorescence.

This dephasing influence is describes as inhomogeneous broadening of the transition and the key parameter is $T_2^*$, which quantifies the time that elapses before Bloch vectors start to lose coherence among them in the system from a fully excited state. [4, p. 523]

The coherence of the system is fundamental; if lost, the system doesn't emit through superfluorescence but behaves as a standard spontaneous emission.

For this reason

$$\tau_R \ll T_2^* \tag{2.34}$$

is necessary to have a superfluorescent pattern [7, p. 1519].

Another condition is due to the extended nature of the system ($d > \lambda$): in order to have a full participation of atoms, the field generated should be able to influence all parts of the system. Due to the finite speed of light, which has to cross the whole length of the system, this requirement translates to:

$$L/c \lesssim \tau_R. \tag{2.35}$$

To make an example in our pencil-shaped sample $L \approx 5\,\text{mm}$ implying $\tau_R >$ ps, well satified in the experiments described in the following.

## 2.5 Rare-earth elements

In this work rare-earth elements are used as medium for generation of superfluorescent beams.

It's worth asking about the reasons for the use of such media. First of all, due to their electronic structure: the orbitals $5s$, $5p$ are complete, while $4f$ is not; this happens because of the high angular momentum, which places $4f$ levels above the other two in terms of energetic ordering; it results that $4f$ active levels are spacially surrounded and shielded from most environmental interactions by $5s$, $5p$ electrons; this particular configuration allows $4f$ level transitions to be good candidates to observe superfluorescence [8, p. 17].

Disturbing interactions on electrons are caused by to different energetic conditions which electrons undergo, which breaks the global symmetry of the system and makes more difficult the creation of the global dipole of the system; the action of close atoms in most cases are caused by electronic and nuclear spin-orbit coupling, hyperfine splitting, phonon transfer in a crystal, atomic scattering energy transfer in gases; the influence of these factors directly acts on the generation of the superfluorescent beams and can be quantified by measuring the inhomogeneous linewidth of the radiation.

A particular case of usage of rare-earth elements is when they are placed into an optical crystal as dopant; the crystal structure helps the system to have a more symmetric structure while having a degree of freedom in choosing the concentration of rare-earth materials. The crystal field also acts as environmental influence on rare-earth electrons by slightly perturbing their energy levels and by making possible to do transitions which would be impossible to observe with pure elements; these transitions lifetimes can be of order of milliseconds and combined with orbital shielding and other crystal effects (like non-Kramers' doublets creation) allow to improve the coherence time a lot [8, p. 17].

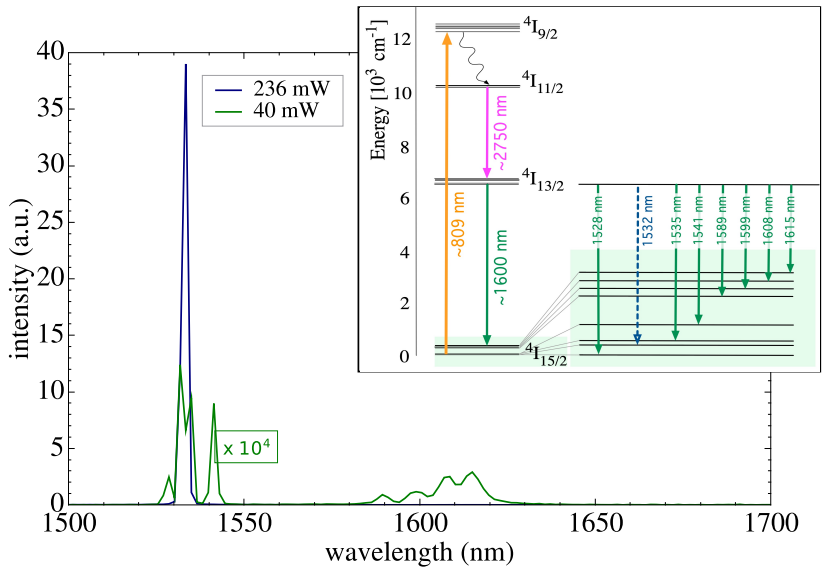


Figure 2.2: $Er^{3+}$:YLF levels taken in account during the experiment; curvy transition is non-radiative; the measured superfluorescent emission is 1532 nm line.

Lastly, crystals are useful purely from the experimental point: unlike gases, which need to be contained by optical interfaces and have a controlled pressure, crystals don't need specific setup to be ready to use in optical experiments and can be managed quite easily.

### 2.5.1 $Er^{3+}$:YLF crystal

A particular rare-earth - crystal configuration was used in this experiment, erbium ion ($Er^{3+}$) with yttrium lithium fluoride matrix ($LiYF_3$), also called $Er^{3+}$:YLF.

The most relevant crystal transitions are observed in the infrared region of the spectrum; in particular, the observed experimental transition used to produce superfluorescence is $^4I_{13/2} \longrightarrow {}^4I_{15/2}$, with a group of multiple transitions localized in 1500 - 1600 nm region.

# Chapter 3

# Experimental

In this part I study and analyse data taken from superfluorescence experiments that take place in Legnaro National Laboratory (INFN-LNL) using a rare-earth doped crystal $Er^{3+}$:YLF as active medium.

In section 3.1 I describe the experimental setup.

I analyse the collected experimental data in section 3.2 by selecting (subsection 3.2.1), filtering (subsection 3.2.2) and fitting with the expected hyperbolic secant squared curve (subsection 3.2.4).

Geometrical and spontaneous emission coefficients are estimated with the available data (subsection 3.2.3) and using the whole information I compare the experimental theoretical and theoretic behaviour, like square dependence of intensity (subsection 3.2.6) and variable superfluorescent peak width behaviour (subsection 3.2.7); I give an estimate of the emitting number of atoms in the sample (subsection 3.2.5).

## 3.1 Description of experimental setup

We have recorded temporal profiles of the emitted photon bunches to experimentally verify the hyperbolic secant squared dependence intensity in time, $1/\sqrt{I}$ dependence of superfluorencent time $\tau_R$ on the photon rate and intensity $N^2$ dependence of the pulses.

The used experimental apparatus (Figure 3.1), as schematically shown in Figure 3.2, includes the following parts:

- The 1% $Er^{3+}$ concentration, 5x5x5 $mm^3$-volume $Er^{3+}$:YLF crystal.
- The continuous wave Ti:sapphire laser, with ring cavity stabilization; the laser is frequency tunable, with $0.1 \times 10^{-3}$ nm wavelength stabilization and 10 MHz linewidth. The maximum input power is 400 mW. The waist width, obtained with knife-edge measurement, is $w = 163\,\mu m$.
- The cryogenic apparatus, composed by superfluid helium-4 that surrounds the crystal and optically interfaces with the external environment; the helium is mantained in a superfluid state at the temperature of 2.17 K, by taking away the gaseous helium, with the use of a pump; in this state the phonon excitation in the crystal is reduced and the bubble formation, that disturbs the optical measurement, is avoided; sensors monitor in real time the helium temperature, heating rate and residual gas pressure.
- The superfluorescent dynamics is investigated with an InGaAs photodiode detector (Thorlabs DET10C responsivity: 1.0 A/W, rise time 10 ns) with input longpass filter with a cut-on wavelength of 1300 nm. The photodiode is connected to an oscilloscope, which records the experimental data (10000 points per each pulse measurement, $\Delta t = 0.05$ ns between two points).

The reported measurement of the laser input wavelength is of 808.992 nm, which is the ${}^4I_{15/2} \longrightarrow {}^4I_{9/2}$ transition from Figure 2.2.

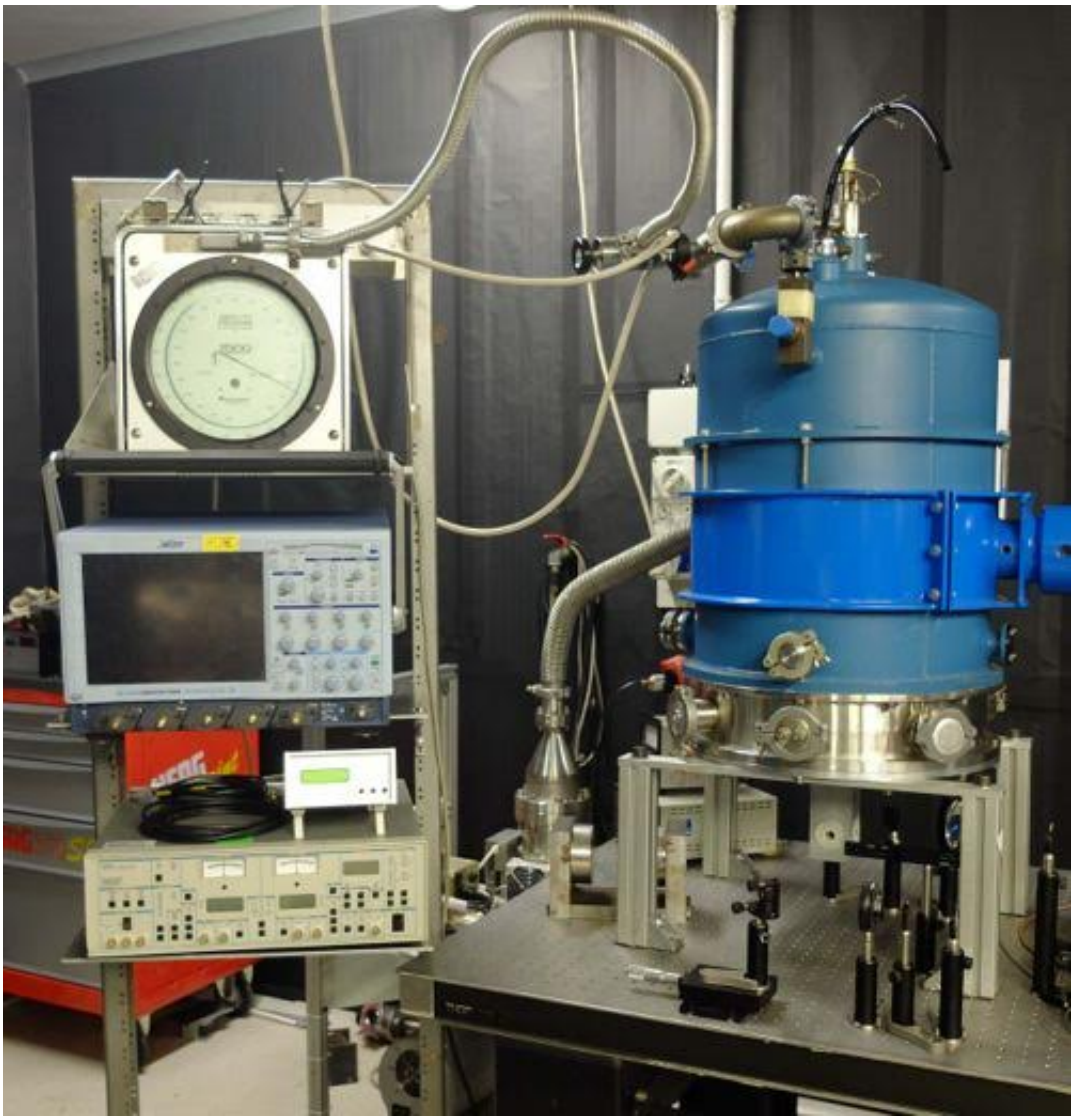

Figure 3.1: Cryogenic and measurement parts of the experimental setup; the window under the cryostat is where the crystal is located during the experiment.

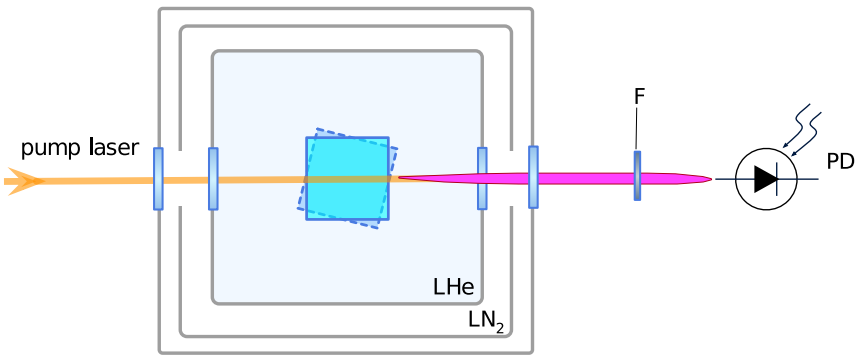


Figure 3.2: Simplified scheme of the experimental setup.

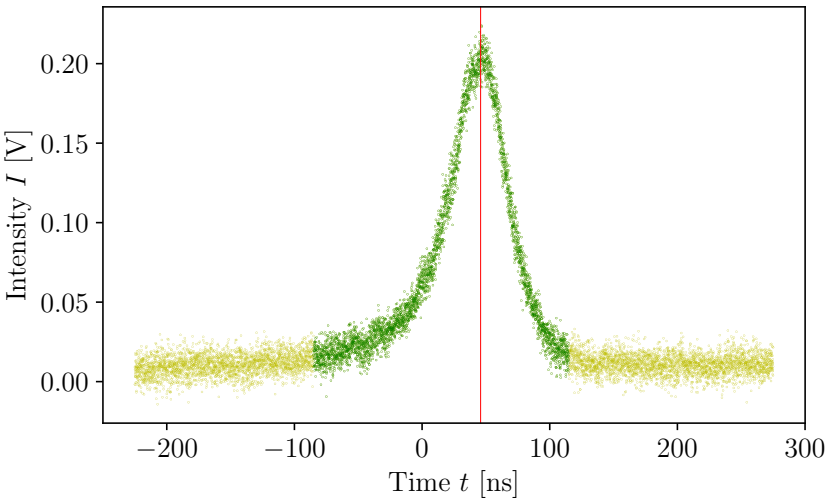


Figure 3.3: One of the extracted superfluorescent peaks by peak detection and cutting algorithms

## 3.2 Data analysis

The experimental data are five time series groups that include 150-320 time series of triggered superfluorescent pulses each; every group is discriminated by input laser power; a time series is a single superfluorescent burst measured by a photodiode and registered by an oscilloscope.

I have applied the analysis procedure to a single group, then replicated for other four.

### 3.2.1 Peak detection and cutting

An algorithm has been used to select and identify the superfluorescent peaks from the data.

The peak detection algorithm selects 101-st to 200-th points with highest $y$ (intensity) values out of 10000, finds their mean $x$ (time) values and translates the data to align the peak time value to 0; this way it makes use of $y$-axis symmetry in the region near the peak while it doesn't consider peak spike values which have an asymmetric and non-uniform distribution of points.

The cutting procedure is done considering the intensity $\langle y_b \rangle$ as the mean intensity of 1500 left and 1500 right points of the time series; then the time interval of 10000 points is divided in 100 points subintervals $I_i = \{(x,y)_{100i+0}, (x,y)_{100i+1}, (x,y)_{100i+2}, \cdots, (x,y)_{100i+99}\}$; for each interval the mean of intensity $\langle y(I_i) \rangle$ as well as the standard deviation $\sigma(y(I_i))$ are calculated; starting from the left and moving forward for each subinterval the condition $\langle y(I_i) \rangle > \langle y_b \rangle + \sigma(y(I_i))$ is checked, the first time it is true the cut is done and data on the right are taken; the same algorithm is applied moving from right to left and taking the remaining data on the left.

This algorithm reduces 10000 points to 2500-4000 depending on the peak width.

### 3.2.2 Ringing elimination

Some peaks in the sample exhibit oscillations, as shown in Figure 3.4. In the literature these oscillations are ascribed to ringing, an inherent process in superfluorescencence [4].

In my analysis I have used only the data without this ringing effect.

The following algorithm is used to find and eliminate peaks with the occurring ringing. First of all the peak is smoothed by applying three times a mean filter by averaging 40 points around each point of the peak; then the data intensity ($I$) is normalized by the peak height (calculated as the mean of intensity coordinates of 50 highest intensity around the peak). A list of differences of intensities is calculated, then this operation is repeated on the last list; at this point their modulus is calculated.

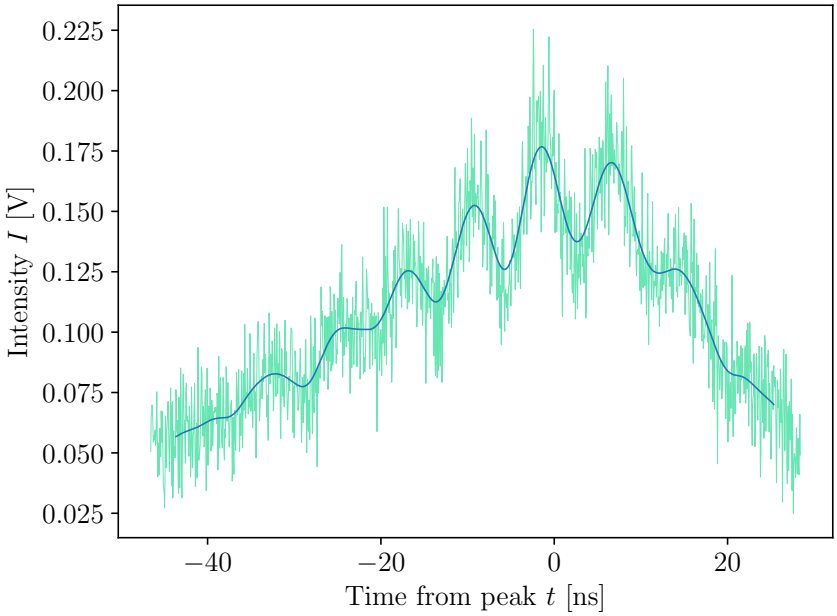


Figure 3.4: One of peaks affected by ringing; the continuous line is data after three applications of the mean filter.

50 largest elements are summed together, if the sum is bigger than a threshold value, then the peak is considered too much irregular and is discarded. This procedure is applied for all peaks.

### 3.2.3 $\mu, \Gamma$ parameters estimation

$\mu$ estimates the geometrical contribution to the superfluorescent lifetime and is dependent on the diffraction angle $\Omega_0$, as reported in Equation 2.31, which gives:

$$\mu = \frac{3}{8\pi^2}\left(\frac{\lambda}{w}\right)^2 = (4.17 \pm 0.04) \cdot 10^{-6}$$

$\Gamma$ rate is calculated as inverse of spontaneous lifetime $T_1 = 15.3$ ms of atoms:

$$\Gamma = \frac{1}{T_1} = \frac{1}{0.0153\,\mathrm{s}} = (65.4 \pm 0.7)\,\frac{1}{\mathrm{s}}$$

As result:

$$\mu\Gamma = (2.72 \pm 0.04) \cdot 10^{-4}\,\frac{1}{\mathrm{s}}$$

### 3.2.4 Peak interpolation

Each filtered superfluorescent peak time series has been interpolated using the form suggested by the theory (Equation 2.33):

$$y = a \cdot \mathrm{sech}^2\,(bt + d) + c \tag{3.1}$$

Example data examples with their interpolations are provided in Figure 3.5. We observe that the stronger the photon emission intensity implies the sharper emission peak. The FWHM of the peaks is approximately 30-60 ns.

Fast pulses have a fall time $\approx 10$ ns and the photodiode has a comparable rise time (10 ns). This may limit the observation of faster pulses in this experiment.

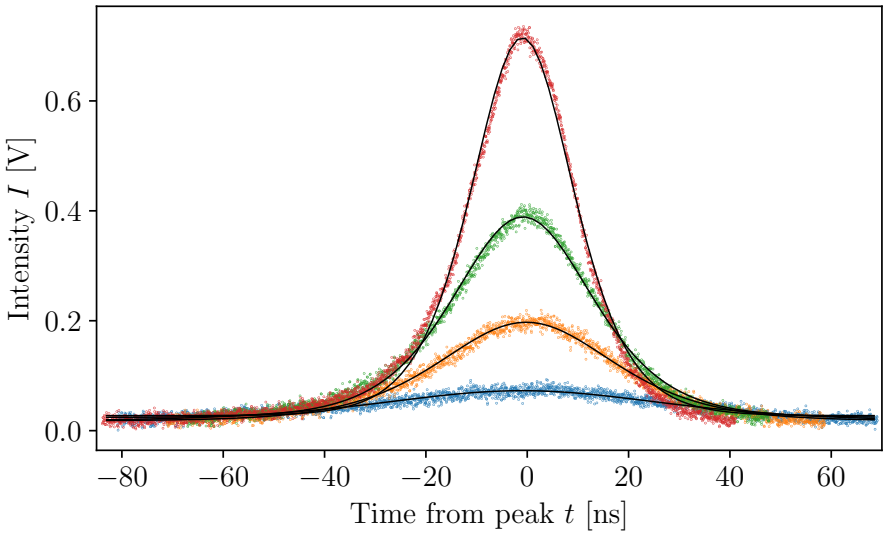


Figure 3.5: Examples with different intensities and peak time widths, $P = 400\,\mathrm{mW}$

### 3.2.5 Estimation of emitted photon number

An estimate of the number of emitted photons is done by applying Equation 2.33.

$$b = \frac{1}{2\tau_R} = \frac{\mu\Gamma N}{2}$$

By using the coefficient $b$ from Equation 3.1 interpolations $N$ is related to all known variables:

$$N = \frac{2b}{\mu\Gamma}$$

Since $b$ is in order of $10^7 - 10^8\,\mathrm{s}^{-1}$, $N \approx 10^{11}$ units (Figure 3.6).

### 3.2.6 Square dependence

With the parameters found in subsection 3.2.4 the verification of the square dependence of intensity ($I$) to a quantity proportional to the number of the partecipating atoms ($N\mu\Gamma$) is possible. Observed data satisfy the parabolic behaviour when fit, as shown in Figure 3.6.

Superfluorescence appears only from a starting value of $N \approx 2 \cdot 10^{11}$ atoms dependent to chosen the crystal and other experimental conditions.

A more suitable form to evaluate time evolution of the superfluorescent emission intensity (Equation 2.33) replaces $N^2$ factor with $N(N - N_0)$:

$$\frac{I}{\hbar\omega_0} = \frac{N(N - N_0)\mu\Gamma}{4}\,\mathrm{sech}^2\left[\frac{1}{2\tau_R}(t - t_D)\right] \tag{3.2}$$

### 3.2.7 $\tau_R$ dependence

The time independent part of Equation 3.2 can be inverted as $\tau_R$ function of intensity $I$ as:

$$\tau_R = \frac{a}{I}\left[1 + \sqrt{1 + bI}\right] \tag{3.3}$$

Data from the interpolation of subsection 3.2.4 are used to evaluate the intensity of the photon emission ($I$) versus the superfluorescent time of pulses ($\tau_R$) and to verify Equation 3.3 by interpolation.

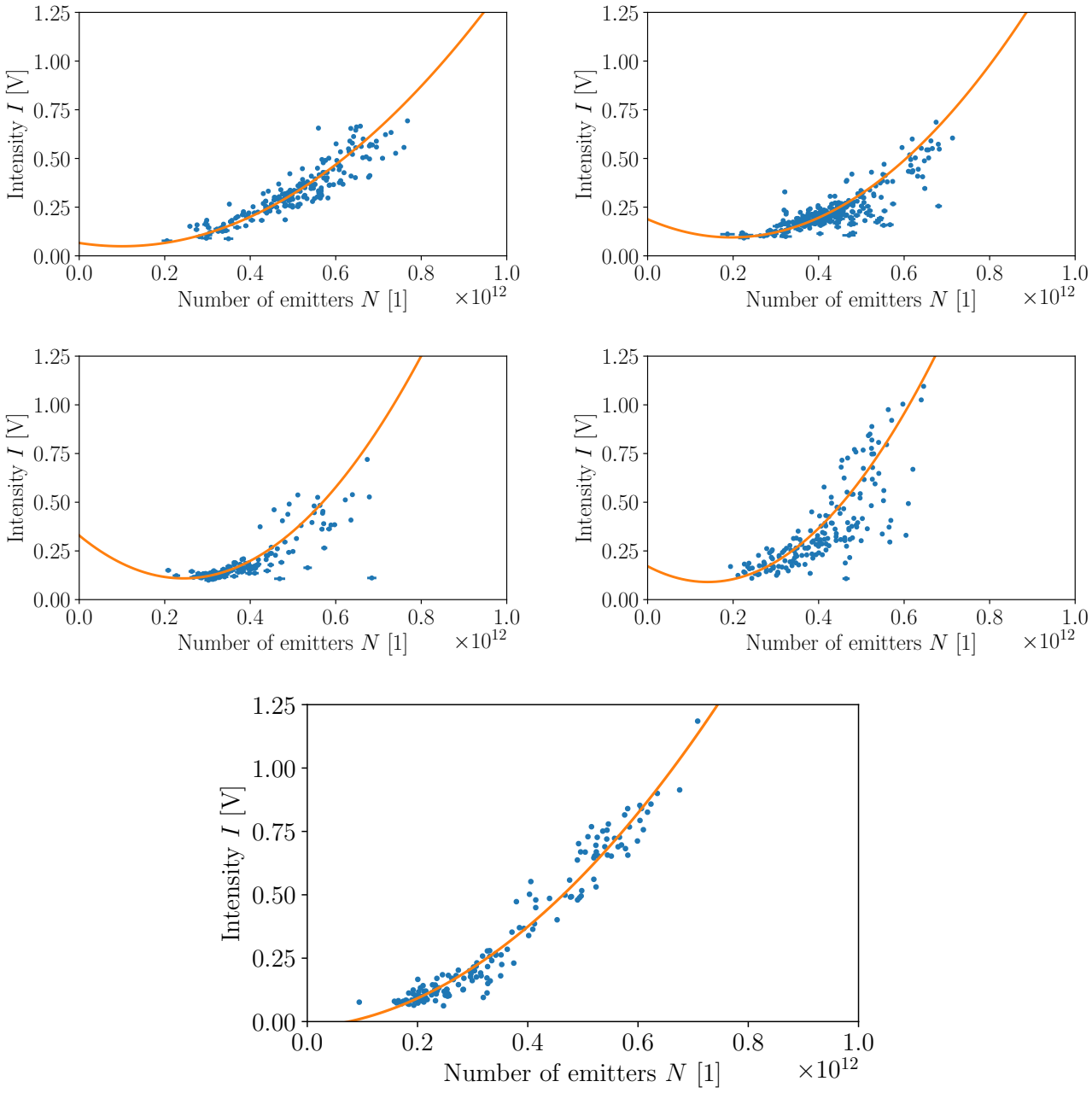


Figure 3.6: Parabolic dependence graph of intensity on $N$ emitting units. The input laser powers are, in order, 208 mW, 280 mW, 356 mW, 400 mW, 400 mW

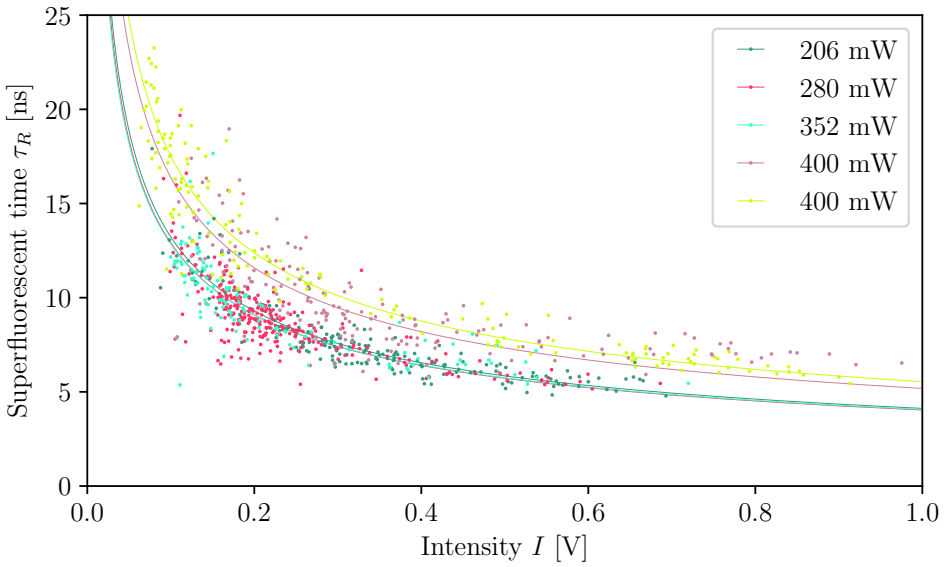


Figure 3.7: Intensity ($I$) vs superfluorescence time ($\tau_R$) graph, different input laser powers are compared.

As shown in Figure 3.7, the superfluorescent time $\tau_R$ distribution is in the range of $5-25$ ns. Compared with the spontaneous emission lifetime of the system $T_1 = 15.3$ ms, this results in an acceleration of $0.6 - 3 \cdot 10^6$ times.

The graph also shows the $\tau_R - I$ dependence is barely affected by the pump laser input power.

# Chapter 4

# Conclusions

Superfluorescence is an electromagnetic emission with a specific temporal characteristics that depend on the number of the participating atoms. These characteristics are totally different compared to the standard spontaneous emission and totally depend on the quantum coherence of the system.

In this work I have analysed experimental data and showed their peculiar superfluorescence characteristics that include:

- the $\mathrm{sech}^2(t)$ temporal evolution of superfluorescent pulses;
- the $N^2$ dependence of the maximum peak intensity on the number of atoms;
- the $1/\sqrt{I}$ dependence of the peak width (superfluorescent time) which being not much dependent on the input laser power;

with different input laser powers. Data reasonably agree with the theoretical results. I also have estimated the number of the participating atoms in the pulses.

Experimental results are in agreement with the presented superfluorescence theory.

# Bibliography


[1] R. H. Dicke. Coherence in spontaneous radiation processes. *Phys. Rev.*, 93(1):99–110, 01 1954.

[2] M. G. Benedict, A. M. Ermolaev, V. A. Malyshev, I. V. Sokolov, and E. D. Trifonov. *Super-radiance Multiatomic coherent emission.* Taylor and Francis Group, 1996.

[3] M. Gross and S. Haroche. Superradiance: An essay on the theory of collective spontaneous emission. *Phys. Rep.*, 93(5):301–396, 1982.

[4] François Auzel. Chapter 151 coherent emission in rare-earth materials. *Handbook on The Physics and Chemistry of Rare Earths*, 22:507–606, 12 1996.

[5] Paul Adrien Maurice Dirac and Niels Henrik David Bohr. The quantum theory of the emission and absorption of radiation. *Proceedings of the Royal Society of London. Series A, Containing Papers of a Mathematical and Physical Character*, 114(767):243–265, 1927.

[6] V. Weisskopf and E. Wigner. Berechnung der natürlichen linienbreite auf grund der diracschen lichttheorie. *Zeitschrift für Physik*, 63(1):54–73, Jan 1930.

[7] R. Bonifacio and L. A. Lugiato. Cooperative radiation processes in two-level systems: Superfluorescence. *Phys. Rev. A*, 11(5):1507–1521, 05 1975.

[8] Andreas Walther. *Coherent Processes in Rare-Earth-Ion-Doped Solids.* PhD thesis, Atomic Physics, 2009.